Electronic Supplementary Material (ESI) for Journal of Materials Chemistry A.


# Supporting Information

# Cascade Charge Transfer Mediated by *In-situ* Interface Modulation Toward Solar Hydrogen Production

Yu-Bing Li,[a] Tao Li,[a] Xiao-Cheng Dai,[a] Ming-Hui Huang,[a] Yunhui He,[b] Guangcan Xiao,[b] Fang-Xing Xiao[a]*

a. College of Materials Science and Engineering, Fuzhou University, New Campus, Minhou, Fujian Province 350108, China.

b. Instrumental Measurement and Analysis Center, Fuzhou University, Fuzhou, 350002, People's Republic of China.

E-mail: fxxiao@fzu.edu.cn

# Table of contents

**Page NO.**



**Note:** The three samples are referred to pristine CdS NWs, CdS@CdSe (25 ℃) and CdS@CdSe-6M (25 ℃), respectively.

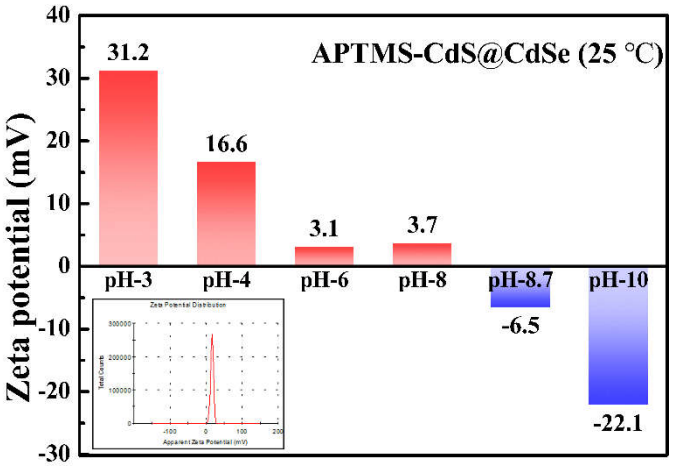


**Fig. S1.** Zeta potentials of APTMS modified-CdS@CdSe (25 ℃) as a function of pH value.

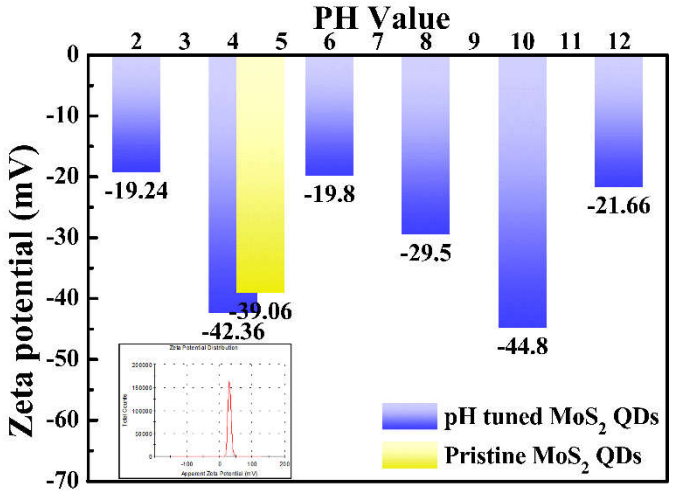


**Fig. S2.** Zeta potentials of $MoS_2$ QDs as a function of pH value.

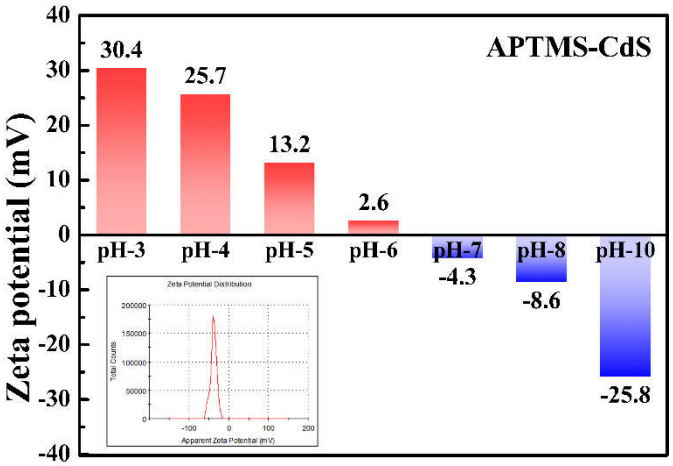


**Fig. S3.** Zeta potentials of APTMS modified CdS NWs as a function of pH value.

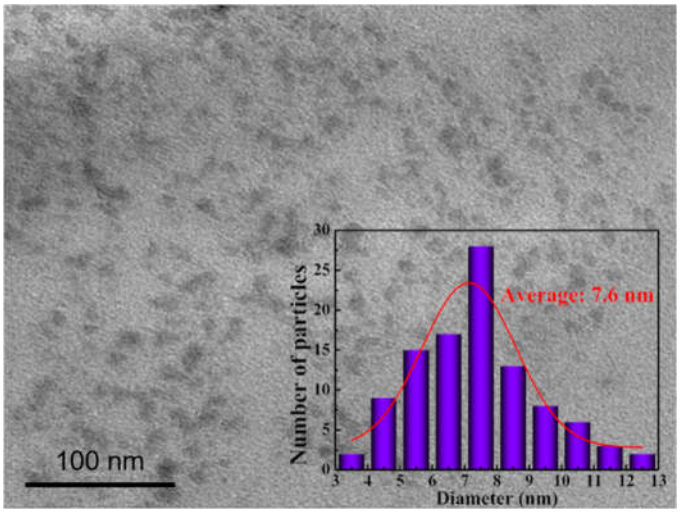


**Fig. S4.** TEM image of $MoS_2$ QDs with corresponding size distribution histogram in the inset.

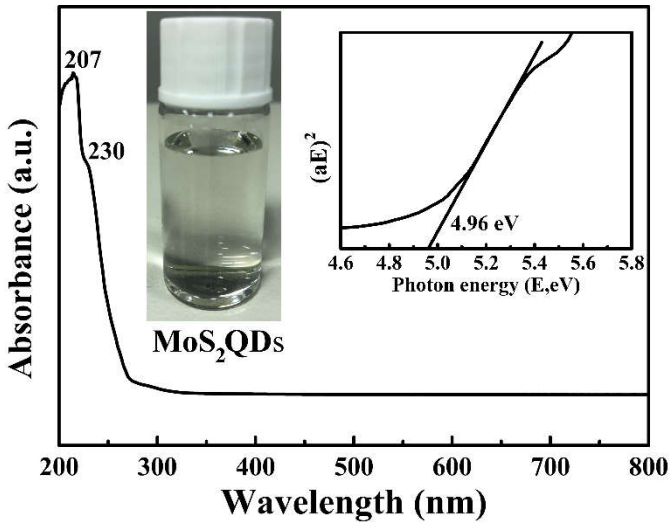


**Fig. S5.** UV-vis absorption spectrum of $MoS_2$ QD aqueous solution with corresponding photograph and band-gap energy in the insets.

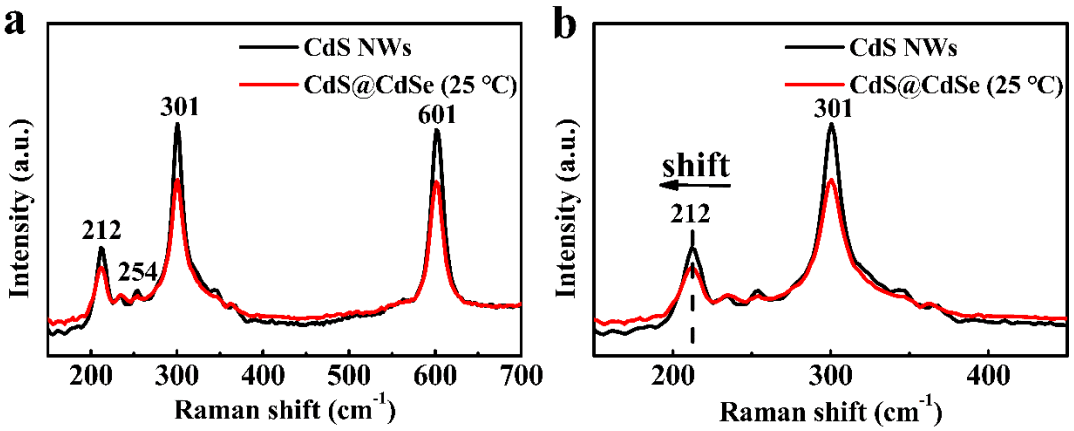


**Fig. S6.** (a) Raman spectra of pristine CdS NWs and CdS@CdSe (25 ºC) with (b) magnified view.

**Table. S1** Peak position with corresponding functional groups.

| *Peak position ($cm^{-1}$)* | *Vibration mode* |
|---|---|
| **3420** | N-H stretching vibration |
| **2925** | C-H stretching vibration |
| **1635** | N-H deformation vibration |
| **1465** | $CH_2$ deformation vibration |
| **1377** | $CH_3$ deformation vibration |
| **1055** | Si-O[S1], C-N stretching vibrations |

**Table. S2** Summary of the specific surface area, pore volume and pore size of blank CdS NWs, CdS@CdSe (25 ℃) and CdS@CdSe-6M (25 ℃).

| *Samples* | *$S_{BET}$ ($m^2\ g^{-1}$)[a]* | *Total pore volume ($cm^3\ g^{-1}$)[b]* | *Average pore size (nm)[c]* |
|---|---|---|---|
| **CdS NWs** | 6.99 | 0.031 | 17.68 |
| **CdS@CdSe** | 15.01 | 0.027 | 7.42 |
| **CdS@CdSe-6M** | 16.26 | 0.030 | 7.35 |

[a] BET surface area is calculated from the linear part of the BET plot.

[b] Single point total pore volume of the pores at $P/P_0 = 0.99$.

[c] Adsorption average pore width (4V/A by BET).

**Table. S3** Chemical bond species *vs.* B.E. for different samples.

| *Element* | *CdS* | *CdS@CdSe (25 ℃)* | *CdS@CdSe-6M (25 ℃)* | *Chemical Bond Species* |
|---|---|---|---|---|
| **C 1s A** | 284.60 | 284.60 | 284.60 | C-C/C-H |
| **Cd $3d_{5/2}$** | 404.15 | 404.95 | 404.80 | $Cd^{2+}$ S2 |
| **Cd $3d_{3/2}$** | 410.90 | 411.75 | 411.50 | $Cd^{2+}$ |
| **S $2p_{3/2}$** | 160.55 | 161.33 | 161.10 | $S^{2-}$ S3 |
| **S $2p_{1/2}$** | 161.70 | 162.75 | 162.35 | $S^{2-}$ |
| **Se 3d** | N.D. | N.D. | 54.30 | $Se^{2-}$ S4 |
| **Mo $3d_{5/2}$** | N.D. | N.D. | 228.07 | $Mo^{4+}$ S5 |
| **Mo $3d_{3/2}$** | N.D. | N.D. | 232.06 | $Mo^{4+}$ |

N.D.: Not Detected.

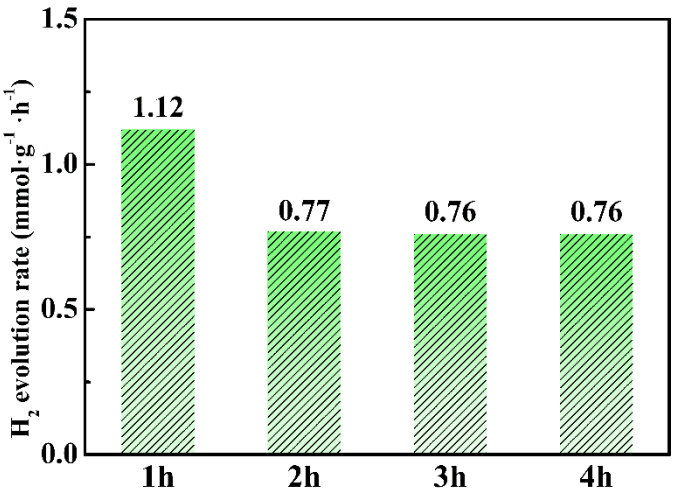


**Fig. S7.** Photocatalytic $H_2$ evolution rate of pristine CdS NWs under visible light irradiation (λ>420 nm).

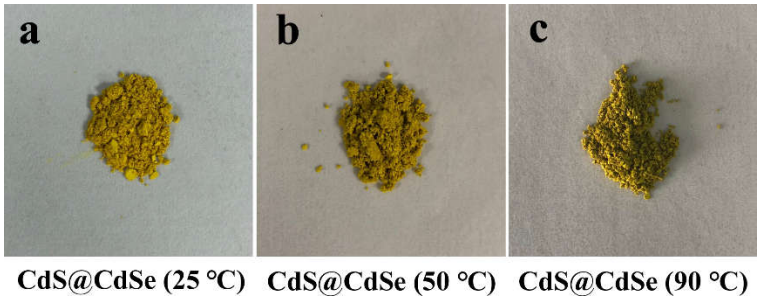


**Fig. S8.** Sample color of CdS@CdSe prepared at different temperature (25, 50, 90 ℃) for triggering *in-situ* phase self-transformation.

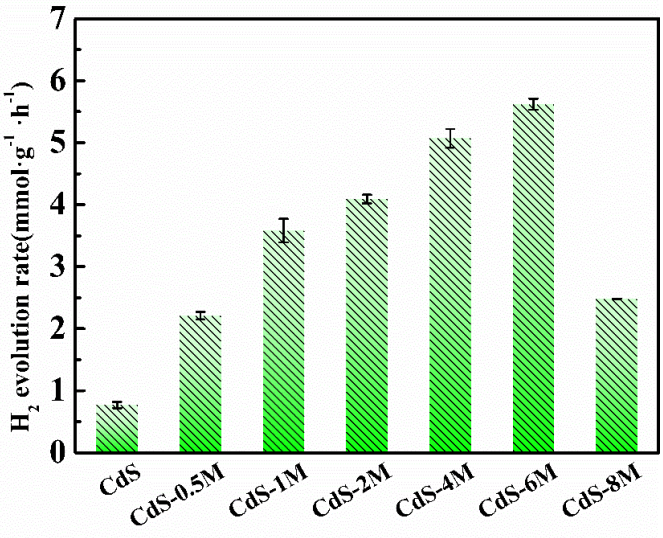


**Fig. S9.** Photocatalytic $H_2$ evolution performances of blank CdS NWs and CdS-X $MoS_2$ (X=0, 0.5, 1, 2, 4, 6, 8 mL) nanocomposites with different adding volumes of $MoS_2$ QDs under visible light irradiation (λ>420 nm).

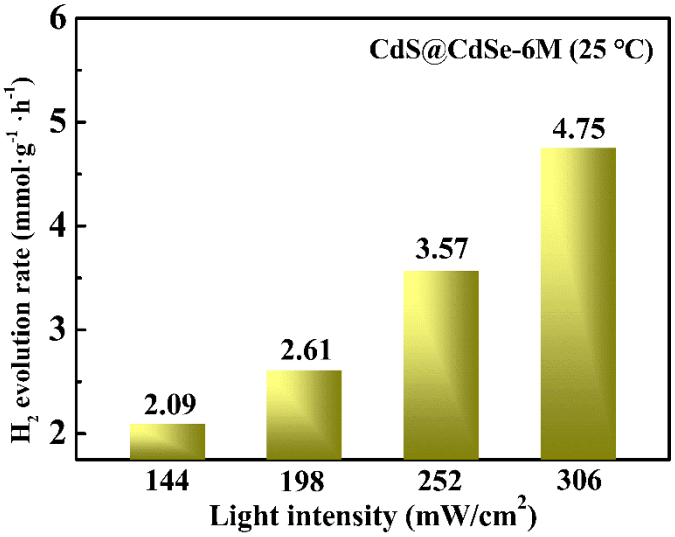


**Fig. S10.** Photocatalytic $H_2$ evolution rates of CdS@CdSe-6M (25 °C) under visible light irradiation (λ>420 nm) with different light intensity (144, 198, 252, 306 mW/cm$^2$).

**Note: Fig. S10** demonstrates that hydrogen production rate increases when the light irradiation intensity gradually boosts, suggesting hydrogen production reaction occurring over CdS@CdSe-6M (25 °C) is indeed caused by a photocatalytic process.

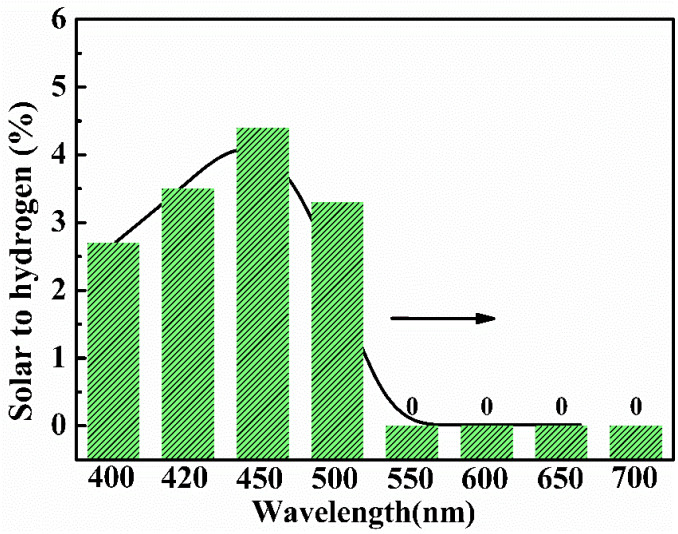


**Fig. S11.** Apparent Quantum yield (A.Q.Y) of CdS@CdSe-6M (25 °C) under different monochromatic wavelengths.

**Table. S4** A.Q.Y of CdS@CdSe-6M (25 °C) and pristine CdS NWs at 450 nm.

| *Photocatalyst* | *Light source* | *Activity (μmol·h$^{-1}$)* | *AQY (%)* |
|---|---|---|---|
| **CdS@CdSe-6M (25 °C)** | 400nm | 9.70 | 2.7 |
| | 420nm | 12.9 | 3.5 |
| | 450nm | 20.7 | 4.4 |
| | 500nm | 17.2 | 3.3 |
| | 550nm | 0 | 0 |
| | 600nm | 0 | 0 |
| | 650nm | 0 | 0 |
| | 700nm | 0 | 0 |
| **CdS** | 450nm | 3.49 | 0.74 |

**Table. S5** S.T.H. of CdS@CdSe-6M (25 ºC) and pristine CdS NWs at 450 nm.

| *Photocatalyst* | *Light source* | *Activity (mmol·g$^{-1}$·h$^{-1}$)* | *S.T.H (%)* |
|---|---|---|---|
| **CdS@CdSe-6M (25 °C)** | 400nm | 0.97 | 26.4 |
| | 420nm | 1.29 | 36.2 |
| | 450nm | 2.07 | 48.7 |
| | 500nm | 1.72 | 40.4 |
| | 550nm | 0 | 0 |
| | 600nm | 0 | 0 |
| | 650nm | 0 | 0 |
| | 700nm | 0 | 0 |
| **CdS** | 450nm | 0.349 | 8.22 |

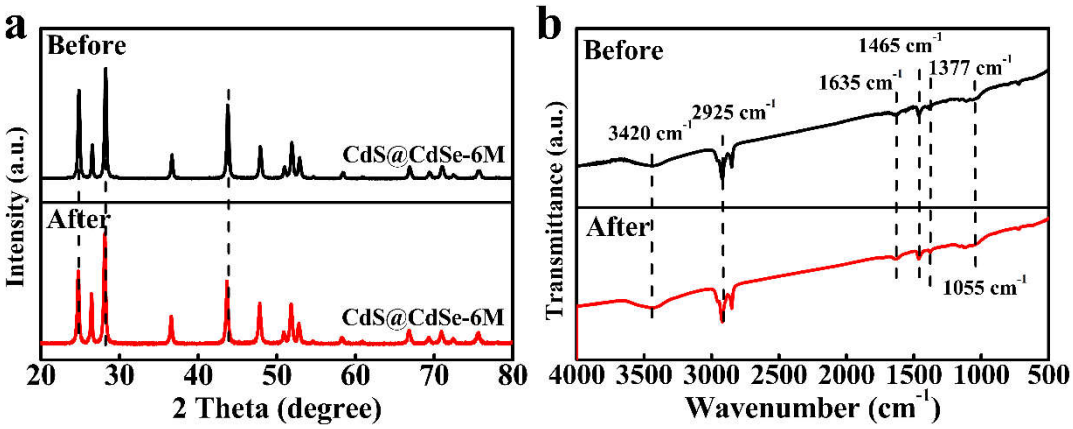


**Fig. S12.** XRD patterns (a) and FTIR spectra (b) of CdS@CdSe-6M (25 °C) before and after cyclic photocatalytic $H_2$ evolution reactions under visible light irradiation (16 h, λ>420 nm).

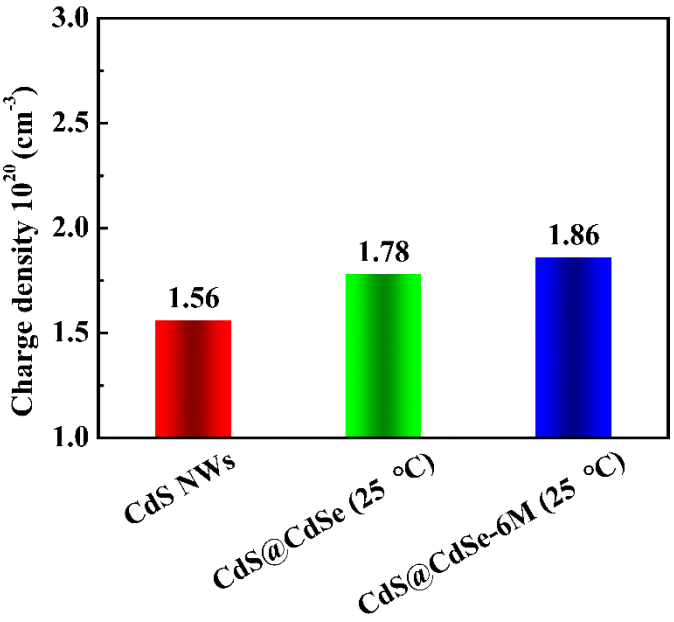


**Fig. S13.** Charge carrier density ($N_D$) of blank CdS NWs, CdS@CdSe (25 °C) and CdS@CdSe-6M (25 °C).

**References**


S1. N. Sadati Behbahani, K. Rostamizadeh, M. R. Yaftian, A. Zamani and H. Ahmadi, *J. Environ. Health Sci. Eng.*, 2014, **12**, 103.

S2. P. R. Nikam, P. K. Baviskar, J. V. Sali, K. V. Gurav, J. H. Kim and B. R. Sankapal, *J. Alloy. Compd.*, 2016, **689**, 394-400.

S3. Z. Yan, X. Yu, A. Han, P. Xu and P. Du, *J. Phys. Chem. C.*, 2014, **118**, 22896-22903.

S4. J. E. B. Katari, V. L. Colvin and A. P. Alivisatos, *J. Phys. Chem.*, 1994, **98**, 4109-4117.

S5. C. Liu, L. Wang, Y. Tang, S. Luo, Y. Liu, S. Zhang, Y. Zeng and Y. Xu, *Appl. Catal. B-Environ.*, 2015, **164**, 1-9.